

EL2-like defects in InP nanowires

R. H. Miwa, and T. M. Schmidt

Instituto de Física, Universidade Federal de Uberlândia, C.P. 593, 38400-902, Uberlândia, MG - Brazil

A. Fazzio

Instituto de Física, Universidade de São Paulo, Brazil

(Dated: January 9, 2022)

We have performed an *ab initio* total energy investigation, within the density functional theory (DFT), of antisite defects in InP nanowires (InPNWs) grown along the [111] direction. Our total energy results indicate that, (i) P antisites (P_{In}) are the most likely antisite defect compared with In antisites (In_P), and (ii) the formation energies of P and In antisites do not depend on the NW diameter. In particular, thin InPNWs, diameters of ~ 13 Å, the P_{In} antisite exhibits a trigonal symmetry, lying at 0.15 Å from the T_d site, followed by a metastable configuration with P_{In} in an interstitial position (1.15 Å from the T_d site). We find a P_{In} -P dissociation energy of 0.33 eV, and there is no EL2-like center for such a thin InPNW. However, EL2-like defects occur by increasing the NW diameter. For diameters of ~ 18 Å, the P_{In} -P dissociation energy increases to 0.53 eV, which is 0.34 eV lower compared with the P_{In} -P dissociation energy for InP bulk phase, 0.87 eV. We mapped the atomic displacements and calculated the relaxation energy, Franck-Condon shift, upon single excitation of P_{In} induced states in InPNW. The formation (or not) of EL2-like defects, P_{In} -P dissociation energy barrier, and the Franck-Condon (FC) energy shift, can be tuned by the NW diameter.

PACS numbers: 71.15.Mb, 71.15.Nc, 71.20.-b

I. INTRODUCTION

Antisite is one of the most studied native defect in III-V compounds, for instance, the EL2 center in GaAs. In a seminal work, Kamińska et al. [1] established that the EL2 center exhibits a tetrahedral symmetry, formed by an isolated As antisite defect (As_{Ga}). Afterward, several experimental [2, 3] as well as theoretical studies [4, 5, 6, 7, 8] have been done aiming to clarify the structural and electronic properties of EL2 defect in GaAs. After more than ten year of investigations, currently there is a general agreement that the stable EL2 center is ruled by an isolated As_{Ga} with T_d symmetry, while the metastable $EL2^M$ structure is attributed to the As_{Ga} atom displaced along the C_{3v} axis.

Its is well known that low temperature growth of other III-V semiconductors, not only GaAs, allows the preparation of highly nonstoichiometric compounds. Indeed, anion antisite defects in InP, P_{In} , has been identified for the first time unambiguously through the electron paramagnetic resonance technique by Kennedy and Wilsey [9]. Dreszer et al. [10], using Hall, high-pressure far-infrared absorption and optically detected magnetic resonance measurements (at low temperature), verified that InP has two dominant donor levels associated with the phosphorus antisite defect. Further investigations, based upon *ab initio* total energy calculations, proposed the formation of P_{In} antisites clusters in InP bulk [11].

The most interesting property on this class of defects is the fact that they also exhibit a clear metastable behavior [4, 12, 13]. A neutral anion-antisite defect in III-V compounds has a stable fourfold and a metastable threefold interstitial configuration, where the anion-antisite

is displaced along the C_{3v} axis [13], similarly to EL2 and $EL2^M$ defects observed in GaAs. This center can be photo-excited into a metastable state, and from which it returns to the ground state by thermal activation. Thus, it is expected a persistent photoconductivity for P_{In} at low temperature.

Nowadays the electronic properties of several materials can be tailored throughout the manipulation/control of their size in the atomic scale. Within this new class of (nano)structured materials, the semiconductors nanowires (NWs) are attracting great deal of interest for future applications in several types of nanodevices. In particular, InP-nanowires (InPNWs) have been considered as a potential structure for fabrication of sensors, light emitting diodes, and field effect transistors [14, 15]. Usually the vapor-liquid-solid mechanism, with a gold particle seed, has been utilized for the growth of these nanostructures [16]. These materials are quasi-one-dimensional with electrons confined perpendicularly to the NW growth direction. They exhibit interesting electronic and optical properties due to quantum confinement effects, viz.: the size dependence of InPNW bandgap [17, 18]. Recent *ab initio* calculations, performed by Li et al. [19], suggested the formation of stable DX center in small GaAs quantum-dots, dot diameter smaller than ~ 15 nm.

It is quite likely the formation of native defects during the NW growth process. Therefore, the structural and electronic properties of those defects are important issues to be addressed, in order to improve our understanding of native defects in quasi-1D semiconducting NW systems.

In this paper we carried out an *ab initio* total energy investigation of antisite defects in InPNWs. We find that the formation of EL2-like defects, antisite dissociation

energy, and the Franck–Condon (FC) energy are ruled by the NW diameter. On the other hand, the antisite formation energies are insensitive to the NW diameter, being P_{In} antisites the most likely defect compared with In_P . At the equilibrium geometry, the P_{In} atom in thin InPNW (diameter of 13 Å) exhibits an energetically stable trigonal symmetry, followed by a metastable configuration with P_{In} in an interstitial position, 1.15 Å from the T_d site. In this case, the P_{In} –P dissociation energy is 0.33 eV. Increasing the NW diameter (13 → 18 Å), we find a P_{In} –P dissociation energy of 0.53 eV, where P_{In} lying on the T_d site represents the energetically most stable configuration. For the InP bulk phase, the P_{In} –P dissociation energy is equal to 0.87 eV. Similarly to the bulk phase, P_{In} in InPNW induces the formation of localized states within the energy bandgap. However, for such a thin NW system, this defect does not exhibit an EL2–like behavior. On the other hand, increasing the NW diameter, EL2–like defects are expected to occur. Finally, within a constrained density functional approach [20], we map the atomic displacements along thin InPNW upon single excitation of P_{In} induced states, and calculate the respective relaxation energy, “Franck–Condon” (FC) shift.

II. THEORETICAL APPROACH

Our calculations were performed in the framework of the density functional theory (DFT) [21], within the generalized gradient approximation due to Perdew, Burke, and Ernzerhof [22]. The electron–ion interaction was treated by using norm–conserving, *ab initio*, fully separable pseudopotentials [23]. The Kohn–Sham wave functions were expanded in a combination of pseudoatomic numerical orbitals [24]. Double zeta basis set including polarization functions (DZP) was employed to describe the valence electrons [25]. The self–consistent total charge density was obtained by using the SIESTA code [26]. The InPNW was modeled within the supercell approach, where the InP bilayers were piled up along the [111] direction with periodicity length of $2\sqrt{3}a$ and diameters of 13 and 18 Å (a represents the optimized lattice constant along the [111] direction of InPNW). The NW surface dangling bonds were saturated with hydrogen atoms. A mesh cutoff of 170 Ry was used for the reciprocal–space expansion of the total charge density, and the Brillouin zone was sampled by using one special \mathbf{k} point. We have verified the convergence of our results with respect to the number and choice of the special \mathbf{k} points. All atoms of the nanowire were fully relaxed within a force convergence criterion of 20 meV/Å.

III. RESULTS AND COMMENTS

Figure 1 presents the atomic structure of thin InPNW, diameter of 13 Å, growth along the [111] direction, top

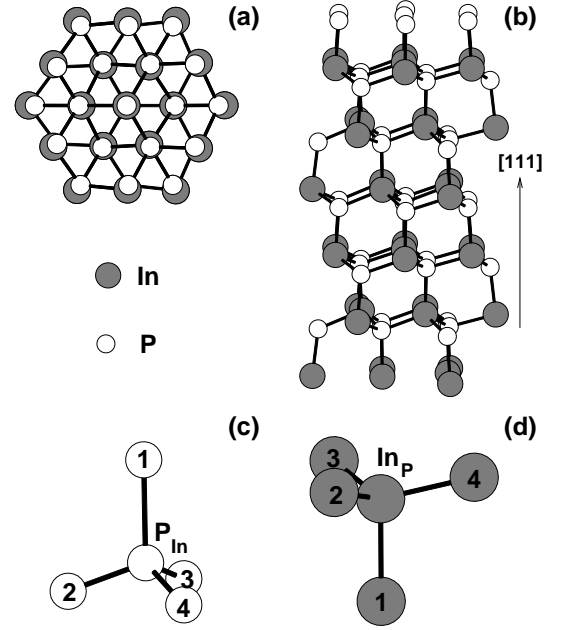


FIG. 1: Structural models of thin InPNW, diameter of 13 Å. (a) Top view and (b) side view. The atomic geometry around the antisite defects are indicated in (c) P_{In} , and (d) In_P .

view [Fig. 1(a)] and side view [Fig. 1(b)] (the hydrogen atoms are not shown). Due to the 1D quantum confinement, perpendicularly to the NW growth direction, the energy gap of InPNW increases compared with the bulk InP (1.0 eV) [18]. We find energy gaps of 2.8 and 2.2 eV for NW diameters of 13 and 18 Å, respectively. It is important to take into account those energy gaps are underestimated, with respect to the experimental measurements, within the DFT approach. Figure 2(a) presents electronic band structure of thin InPNW for wave vectors parallel to the [111] direction (ΓL direction). At the Γ point, the highest occupied states exhibit an energy split of 0.31 and 0.20 eV ($a_1 + e$), for NW diameter of 13 and 18 Å, respectively. The valence band maximum of bulk InP is described by a three–fold degenerated t_2 state. Such ($t_2 \rightarrow a_1 + e$) energy splitting is due to the $T_d \rightarrow C_{3v}$ symmetry lowering of InPNW with respect to the bulk phase.

The energetic stability of antisites in InPNWs can be examined by the calculation of formation energies (Ω_i). The formation energy of P and In antisites, P_{In} [Fig. 1(c)] and In_P [Fig. 1(d)], respectively, can be written as,

$$\Omega_i = E[InPNW_i] - E[InPNW] - n_{In}\mu_{In} - n_P\mu_P.$$

We have considered the formation of antisites in InPNWs. $E[InPNW_i]$ represents the total energy of InPNW with $i = P_{In}$ or In_P antisite defect, and $E[InPNW]$ is the total energy of a perfect InPNW. n_{In} (n_P) denotes the number of In (P) atoms in excess or in deficiency. The In and P chemical potentials, μ_{In} and μ_P , respectively, are constrained by following thermodynamic equilibrium condition, $\mu_{In} + \mu_P = \mu_{InP}^{Bulk}$, where μ_{InP}^{Bulk} is

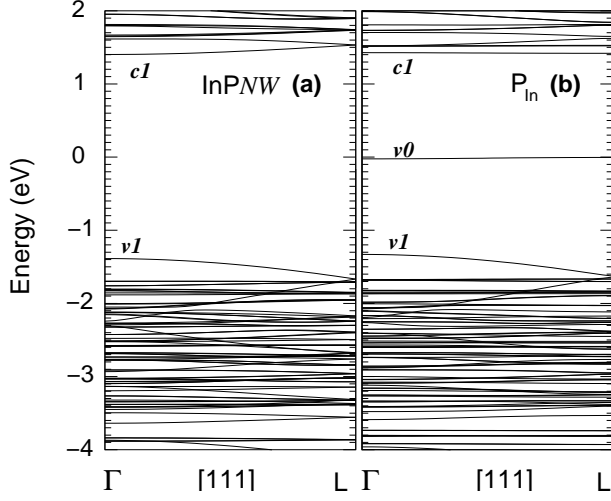


FIG. 2: Electronic band structures of (a) perfect thin InPNW, and (b) defective thin InPNW with a P antisite (P_{In}). NW diameter of 13 Å.

the chemical potential of bulk InP. Under In rich (P poor) condition we will have $\mu_{\text{In}} \rightarrow \mu_{\text{In}}^{\text{Bulk}}$, whereas under In poor (P rich) condition, $\mu_{\text{In}} \rightarrow \mu_{\text{In}}^{\text{Bulk}} - \Delta H_f(\text{InP})$ [27]. For the heat of formation of bulk InP, $\Delta H_f(\text{InP})$, we have considered its experimental value, 0.92 eV.

Figure 3 presents our calculated results of Ω_i for thin InPNW (diameter of 13 Å), as a function of the In chemical potential. It is clear that the formation of P_{In} is dominant compared with In_P. This latter defect occurs only for In rich condition. At the In and P stoichiometric condition (dashed line in Fig. 3) we obtained $\Omega_{\text{P}_{\text{In}}} = 2.15$ eV and $\Omega_{\text{In}_{\text{P}}} = 3.57$ eV. Increasing the NW diameter (18 Å), we find $\Omega_{\text{P}_{\text{In}}} = 2.18$ eV. Within the same calculation procedure, we obtained similar formation energy results for the InP bulk phase, viz.: $\Omega_{\text{P}_{\text{In}}} = 2.14$ eV and $\Omega_{\text{In}_{\text{P}}} = 3.59$ eV. Those results indicate that, (i) there is an energetic preference of P_{In} antisites, compared with In_P, for both structural phases of InP. (ii) The formation energy of P_{In} does not depend on the NW diameter.

At the equilibrium geometry, P_{In} defect in bulk InP keeps the T_d symmetry with P_{In}-P bond lengths of 2.49 Å, while In_P exhibits a weak Jahn-Teller distortion along the [001] direction. Those results are in accordance with previous *ab initio* studies of antisites in InP [11, 28, 29]. On the other hand, the equilibrium geometry of antisites in thin InPNW is quite different. The P_{In}-P₁ bond, parallel to the NW growth direction, is stretched by 27% compared with the other three P_{In}-P_i bonds, $i = 2 - 4$ in Fig. 1(c). Similarly for the In_P antisites, In_P-In₁ is stretched by 8.6% compared with the other three In_P-In bonds indicated in Fig. 1(d). Figures 4(a) and 4(b) depict the total charge densities along the P_{In}-P₁ and In_P-In₁ bonds, respectively. In particular, due to the large P_{In}-P₁ bond stretching, P_{In} is weakly bonded to P₁, whereas the other P_{In}-P₂, -P₃ and -P₄ bonds [see Fig. 4(a)] exhibit a strong covalent character. Therefore,

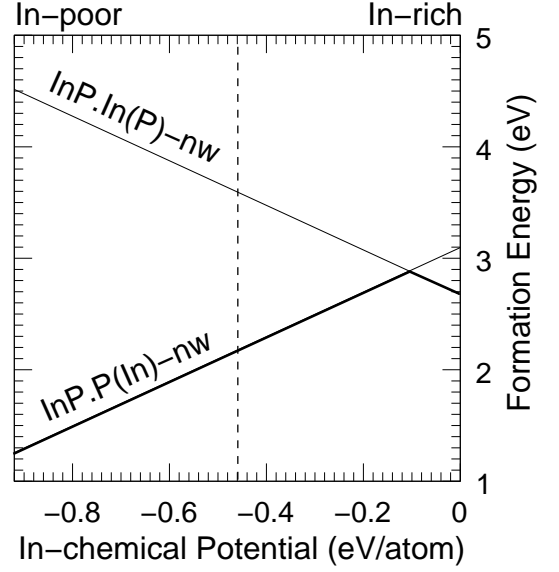


FIG. 3: Formation energies of P_{In} and In_P antisites in thin InPNW, diameter of 13 Å, as a function of In chemical potential.

different from bulk InP, P_{In} antisites in NW system exhibits a C_{3v} symmetry, with the P_{In} atom displaced from T_d site by 0.15 Å along the [111] axis. Such a P_{In} displacement, along the C_{3v} axis, has not been observed by increasing the NW diameter to 18 Å. In this case, the P_{In} atom occupies a T_d site and the P_{In}-P bond lengths are equal to 2.94 Å.

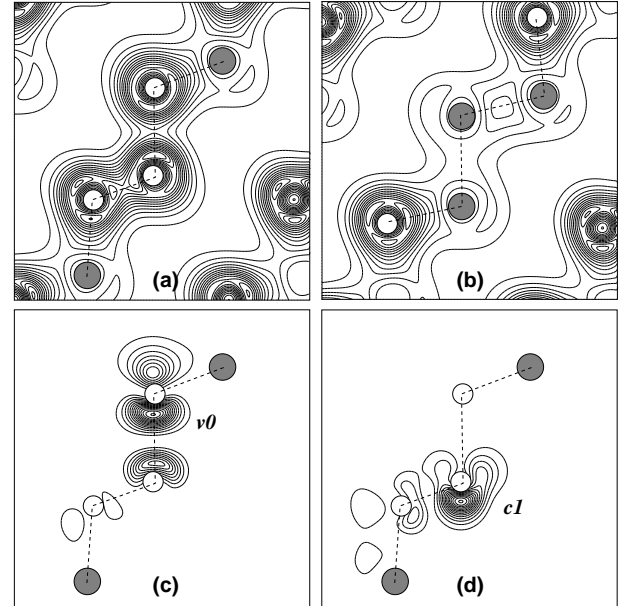


FIG. 4: Total charge densities of (a) P_{In}, and (b) In_P antisites in InPNW. The partial charge densities of P_{In} induced (c) highest occupied $v0$ and (d) lowest unoccupied $c1$ states.

Several anion antisite defects in III-V materials were

studied by Caldas et al. [13]. In that work, based upon *ab initio* total energy calculations, the authors observed an energetically stable T_d symmetry for P_{In} and a metastable C_{3v} configuration for the antisite atom displaced by ~ 1.3 Å along the [111] direction. Indeed, in Fig. 5(a) we present our total energy results as a function of P_{In} displacement, along the [111] direction, for the InP bulk phase. We find that the T_d symmetry represents the energetically most stable configuration, followed by an energy barrier of 0.87 eV at 0.7 Å from the T_d site, $z = 0.7$ Å, breaking the $P_{In}-P_1$ bond. Finally, the metastable C_{3v} configuration occurs for $z = 1.2$ Å, where the P_{In} occupies an interstitial site. Figures 5(b) and 5(c) present the energy barrier for P_{In} in thin InPNW. We have examined two different processes: (i) the In and P atoms of the NW are not allowed to relax during the P_{In} displacement [Fig. 5(b)]. (ii) The In and P coordinates are fully relaxed for each P_{In} step along the [111] direction, i.e. an adiabatic process [Fig. 5(c)]. It is noticeable that the energy barrier calculated in (i) is very similar to that obtained for P_{In} in bulk InP [Fig. 5(a)]. In (i) the energetically most stable configuration for P_{In} exhibits a T_d symmetry, and we find a dissociation energy of 0.84 eV for $z = 0.86$ Å. Further P_{In} displacement indicates a C_{3v} metastable geometry for $z \approx 1.15$ Å, where the P_{In} atom occupies an interstitial site. Meanwhile, in (ii) the C_{3v} symmetry, with the P_{In} atom lying at 0.15 Å from the T_d site, represents the energetically most stable configuration. The $P_{In}-P_1$ dissociation energy reduces to 0.33 eV (at $z = 0.85$ Å), and there is a metastable geometry for $z \approx 1.15$ Å. The total energy difference between the stable (S) and the metastable (M) configurations, $E(S) - E(M)$, in InPNW is equal to -0.084 eV, while in bulk InP we find $E(S) - E(M) = -0.53$ eV. Comparing (i) and (ii) we verify that the atomic relaxation plays a fundamental rule not only to the energy barrier for the P_{In} atomic displacement along the [111] direction, but also for the equilibrium geometry of the P_{In} structure. Increasing the NW diameter, the energy barrier for P_{In} displacement will become similar to that obtained for bulk InP (an upper limit for very large NW diameter), see Fig. 5(d). Indeed, for NW diameter of 18 Å, we find a $P_{In}-P_1$ dissociation energy of 0.53 eV, and $E(S) - E(M)$ equal to -0.14 eV. Those results indicate that the $P_{In}-P_1$ dissociation barrier, and the $E(S) - E(M)$ total energy difference, can be tuned within the shaded region indicated in Fig. 5(d).

Focusing on the electronic structure, the formation of P_{In} defect in thin InPNW gives rise to a deep double donor state, labeled $v0$ in Fig. 2(b), lying at 1.3 eV above $v1$. Such a P_{In} induced state is very localized within the fundamental band gap, being almost flat along the ΓL direction. For P_{In} in bulk InP, *ab initio* studies performed by Seitsonen et al. [28] indicates the formation of an occupied state at 0.7 eV above the valence band maximum. The partial charge density contour plot of $v0$, Fig. 4(c), shows an anti-bonding π^* orbital concentrated along the $P_{In}-P_1$ bond. The lowest unoccupied state, $c1$, is also

concentrated on the P_{In} antisite, as depicted in Fig. 4(d).

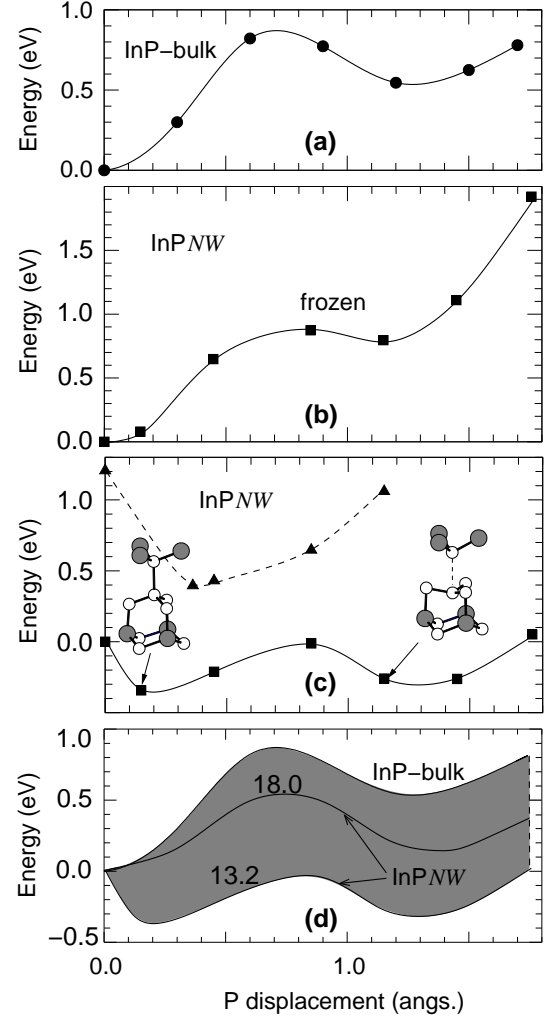


FIG. 5: Total Energy as a function of the P_{In} antisite displacement along the [111] direction: (a) bulk InP, and (b) InPNW where the In and P atoms are not allowed to relax during the P_{In} displacement. (c) Whole In and P atomic position along the NW are allowed to relax. In (c) the total energy barrier indicated by triangles (dashed line) was calculated for an excited electronic configuration, single excitation. (d) Energy barriers for bulk InP and thin InPNW systems.

EL2 and $EL2^M$ centers in III-V are characterized by a stable T_d and a metastable C_{3v} geometries for an isolated V_{III} interstitial atom. However, before the V_{III} antisite arrives to the metastable C_{3v} configuration, there is a strong electronic coupling between the highest occupied and the lowest unoccupied antisite induced states near to the local maximum for the $V_{III}-V$ dissociation energy, see Fig. 3 in Ref. [13] and Fig. 4 in Ref. [30].

Similarly, for thin InPNW, we examined the energy positions of single particle eigenvalues, $\epsilon(v0)$ and $\epsilon(c1)$, as a function of the P_{In} displacement along the C_{3v} axis. Our calculated results, depicted in Fig. 6, reveal that there is no electronic coupling between $v0$ and $c1$. Thus,

based upon the calculated energy barrier [Fig. 5(c)], and the evolution of the antisite induced states, $v0$ and $c1$, we can state that there is no EL2-like center in thin InPNWs. On the other hand, increasing the NW diameter [Fig. 5(d)], EL2-like center is expected to occur in InP.

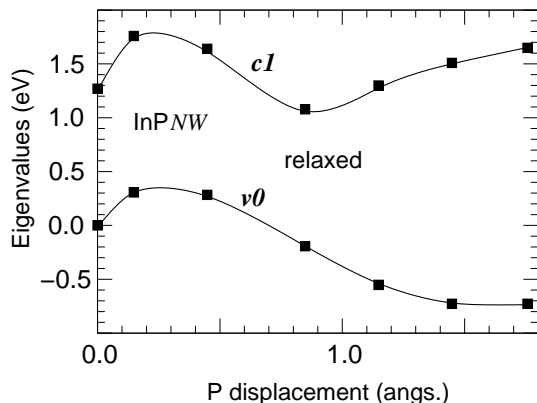


FIG. 6: Single particle eigenvalues (ϵ) for P_{In} : highest occupied $v0$ [Fig. 4(c)] and lowest unoccupied $c1$ [Fig. 4(d)].

Within the DFT approach, we have examined the structural relaxations upon single excitation from the highest occupied state ($v0$) to the lowest unoccupied state ($c1$) of P_{In} in thin InPNW. We have used the calculation procedure proposed by Artacho et al., where the single excitation was modeled by “promoting an electron from the highest occupied molecular orbital (HOMO) to the lowest unoccupied molecular orbital (LUMO)” [20], i.e. a “constrained” DFT calculation. So that, promoting one electron from $v0$ to $c1$, $v0 \rightarrow c1$, we obtained the equilibrium geometry (full relaxations) as well as the self-consistent electronic charge density. The atomic relaxations along thin InPNW, upon $v0 \rightarrow c1$ single excitation, are localized near to the P_{In} position. Since we are removing one electron from the anti-bonding π^* orbital depicted in Fig. 4(c), the $P_{In}-P_1$ bond shrinks by 0.12 \AA ($2.90 \rightarrow 2.78 \text{ \AA}$), and there is radial a contraction of $\sim 0.2 \text{ \AA}$ at $z = 6.8 \text{ \AA}$.

The structural relaxations are proportional to the degradation of optical energy due to the atomic displacements associated with such a $v0 \rightarrow c1$ single excitation, FC shift. Comparing the radial and the longitudinal dis-

placements, we verify that the most of the FC shift comes from the atomic relaxation parallel to the NW growth direction. The atomic displacements along the radial direction (Δr) are localized nearby P_{In} , lying within an interval of $-0.2 < \Delta r < 0 \text{ \AA}$. While the atomic displacements parallel to the growth direction (Δz) lie within a range of $-0.2 < \Delta z < 0.3 \text{ \AA}$, being less concentrated around the P_{In} antisite position. We find a FC energy shift of 0.8 eV , which is quite large compared with the InP bulk phase. Within the same calculation approach, we find a FC energy shift of 0.05 eV for InP bulk. Previous *ab initio* study indicates a FC energy shift of 0.1 eV for bulk InP. Thus, suggesting that the FC energy shift also can be tuned by controlling the NW diameter.

IV. CONCLUSIONS

In summary, we have performed an *ab initio* total energy investigation of antisites in InPNW. We find that the P_{In} antisite is the most likely to occur. For thin InPNWs the P_{In} atom exhibits a trigonal symmetry, followed by a metastable P interstitial configuration. Increasing the NW diameter (18 \AA), P_{In} occupying the T_d site becomes the energetically most stable configuration. The calculated energy barrier, for P_{In} displacement along the C_{3v} axis, indicates that there is no EL2-like defect in thin InPNWs. However, increasing the NW diameter, $13 \rightarrow 18 \text{ \AA}$, we observe the formation of EL2-like defects in InP. Within a “constrained” DFT approach, we calculated the structural relaxations and the FC energy shift upon single excitation of the electronic states induced by P_{In} . We inferred that not only the formation (or not) of EL2-like defects, but also (i) the $P_{In}-P$ dissociation energy, (ii) the total energy difference between stable and metastable P_{In} configurations, $E(S) - E(M)$, and the (iii) FC energy shift can be tuned by controlling the InPNW diameter.

Acknowledgments

The authors acknowledge financial support from the Brazilian agencies CNPq, FAPEMIG, and FAPESP. The most of calculations were performed using the computational facilities of the Centro Nacional de Processamento de Alto Desempenho/CENAPAD-Campinas.

-
- [1] M. Kamińska, M. Skowroński, and W. Kuszko, Phys. Rev. Lett. **55**, 2204 (1985).
 - [2] H. J. von Bardeleben, D. Stiévenard, D. Deresmes, A. Huber, and J. C. Bourgoin, Phys. Rev. B **34**, 7192 (1986).
 - [3] D. Kabiraj and S. Ghosh, Appl. Phys. Lett. **87**, 252118 (2005).
 - [4] D. J. Chadi and K. J. Chang, Phys. Rev. Lett. **60**, 2187 (1988).
 - [5] J. Dabrowski and M. Scheffler, Phys. Rev. Lett. **60**, 2183 (1988).
 - [6] Q.-M. Zhang and J. Bernholc, Phys. Rev. B **47**, 1667 (1993).
 - [7] D. J. Chadi, Phys. Rev. B **68**, 193204 (2003).
 - [8] H. Overhof and J.-M. Spaeth, Phys. Rev. B **72**, 115205 (2005).
 - [9] T. Kenedy and N. Wilsey, Appl. Phys. Lett. **44**, 1089 (1984).

- [10] P. Dreszer, W. M. Chen, K. Seendripu, J. A. Wolk, W. Walukiewicz, B. W. Liang, C. W. Tu, and E. R. Weber, Phys. Rev. B **47**, 4111 (1993).
- [11] T. Schmidt, R. Miwa, A. Fazzio, and R. Mota, Phys. Rev. B **60**, 16475 (1999).
- [12] J. Mikucki, M. Baj, D. Wasik, W. Walukiewicz, W. G. Bi, and C. W. Tu, Phys. Rev. B **61**, 7199 (2000).
- [13] M. J. Caldas, J. Dabrowski, A. Fazzio, and M. Scheffler, Phys. Rev. Lett. **65**, 2046 (1990).
- [14] J. Wang, M. S. Gudiksen, X. Duan, Y. Cui, and C. M. Lieber, Science **293**, 1455 (2001).
- [15] X. Duan, Y. Huang, Y. Cui, J. Wang, and C. M. Lieber, Nature **409**, 66 (2001).
- [16] S. Bhunia, T. Kawamura, Y. Watanabe, S. Fujikawa, and K. Tokushima, Appl. Phys. Lett. **83**, 3371 (2003).
- [17] H. Yu, J. Li, L. Richard A, L.-W. Wang, and W. Buhro, Nat. Mater. **2**, 517 (2003).
- [18] T. M. Schmidt, R. H. Miwa, P. Venezuela, and A. Fazzio, Phys. Rev. B **72**, 193404 (2005).
- [19] J. Li, S.-H. Wei, and L.-W. Wang, Phys. Rev. Lett. **94**, 185501 (2005).
- [20] E. Artacho, M. Rohlfing, M. Côté, P. D. Haynes, R. J. Needs, and C. Molteni, Phys. Rev. Lett. **93**, 116401 (2004).
- [21] P. Hohenberg and W. Kohn, Phys. Rev. **136**, B864 (1964).
- [22] J. P. Perdew, K. Burke, and M. Ernzerhof, Phys. Rev. Lett. **77**, 3865 (1996).
- [23] L. Kleinman and D. M. Bylander, Phys. Rev. Lett. **48**, 1425 (1982).
- [24] O. F. Sankey and D. J. Niklewski, Phys. Rev. B **40**, 3979 (1989).
- [25] E. Artacho, D. Sánchez-Portal, P. Ordejón, A. Garcia, and J. M. Soler, Status Solid B **215**, 809 (1999).
- [26] J. M. Soler, E. Artacho, J. D. Gale, A. García, J. Junquera, P. Ordejón, and D. Sánchez-Portal, J. Phys.: Condens. Matter **14**, 2745 (2002).
- [27] G.-X. Qian, R. M. Martin, and D. J. Chadi, Phys. Rev. B **38**, 7649 (1988).
- [28] A. P. Seitsonen, R. Virkkunen, M. J. Puska, and R. M. Nieminen, Phys. Rev. B **49**, 5253 (1994).
- [29] C. W. M. Castleton and S. Mirbt, Phys. Rev. B **70**, 195202 (2004).
- [30] J. Dabrowski and M. Scheffler, Phys. Rev. B **40**, 10391 (1989).